

Dramatic changes in the horizontal structure of mangrove forests in the largest delta of the northern Beibu Gulf, China

Riming Wang¹, Zhijun Dai^{2*}, Hu Huang^{1*}, Xixing Liang^{1, 2}, Xiaoyan Zhou², Zhenming Ge², Baoqing Hu³

¹ Guangxi Key Laboratory of Marine Environmental Change and Disaster in Beibu Gulf /Beibu Gulf Ocean Development Research Center, Beibu Gulf University, Qinzhou 535011, China

² State Key Laboratory of Estuarine and Coastal Research, East China Normal University, Shanghai 200062, China

³ Key Laboratory of Environment Change and Resources Use in Beibu Gulf (Nanning Normal University), Ministry of Education, Nanning 510310, China

Received 4 June 2022; accepted 17 October 2022

© Chinese Society for Oceanography and Springer-Verlag GmbH Germany, part of Springer Nature 2023

Abstract

The horizontal structure of mangrove forests is an important characteristic that reflects a significant signal for coupling between mangroves and external drivers. While the loss and gain of mangroves has received much attention, little information about how the horizontal structure of mangrove forests develops from the seedling stage to maturity has been presented. Here, remote sensing images taken over approximately 15 years, UVA images, nutrient elements, sediments, and *Aegiceras corniculatum* vegetation parameters of the ecological quadrats along the Nanliu Delta, the largest delta of the northern Beibu Gulf in China, are analyzed to reveal changes in the horizontal structure of mangroves and their associated driving factors. The results show that both discrete structures and agglomerated structures can often be found in *A. corniculatum* seedlings and saplings. However, the combination of seedlings growing into maturity and new seedlings filling in available gaps causes the discrete structure of *A. corniculatum* to gradually vanish and the agglomerate structure to become stable. The aggregated structure of seedlings, compared to the discrete structure, can enhance the elevation beneath mangroves by trapping significantly more sediments, providing available spaces and conditions for seedlings to continue growing. Furthermore, by catching fine sediments with enriched nutrients, the survival rate of *A. corniculatum* seedlings in the agglomerated structure can be much higher than that in the discrete structure. Our results highlight the significance of the agglomeration of *A. corniculatum*, which can be beneficial to coastal mangrove restoration and management.

Key words: deltaic mangrove, *Aegiceras corniculatum*, horizontal structure, biomorphodynamic processes, Nanliu Delta

Citation: Wang Riming, Dai Zhijun, Huang Hu, Liang Xixing, Zhou Xiaoyan, Ge Zhenming, Hu Baoqing. 2023. Dramatic changes in the horizontal structure of mangrove forests in the largest delta of the northern Beibu Gulf, China. Acta Oceanologica Sinica, 42(7): 116–123, doi: 10.1007/s13131-022-2126-x

1 Introduction

Mangroves grow in tropical and subtropical shorelines, providing significant ecological, economic and societal benefits to humans (Lovelock et al., 2015). However, mangroves have been threatened with large-scale losses by anthropogenic drivers and sea level rise (Mishra et al., 2021). Approximately 38 200 hm² across the globe has disappeared in the last decade (FAO, 2020). It is expected that mangroves could rapidly decrease in number due to lasting human interference (Friess et al., 2019). While sea level rise caused by global warming is a potential threat to mangrove ecosystems (Lovelock et al., 2015), sufficient sediment supply from rivers enables mangrove forests to grow due to their native biomorphodynamic features, which give them the capacity to cope with sediment (Lovelock et al., 2017; Woodroffe et al., 2016). Furthermore, the supply of fluvial suspended sediment, changes in the local suspended sediment concentration, and the relation-

ship between estuarine hydrodynamics and mangrove forest ecosystems will induce losses or gains in global mangrove forests. When the local suspended sediment concentration remains almost unchanged with the decline in sediment discharge from upstream, mangrove forests can maintain seaward horizontal growth (Long et al., 2021). Mangroves can accelerate tidal flat silting by reducing waves and promoting sediment deposition. During a catastrophic tsunami, a 100-m-wide belt of mangroves with 30 trees per 100 m² can reduce flow pressure by 90% (Danielsen et al., 2005), and a mild slope along mangrove tidal flats can reduce wave energy by 93%–98% (Parvathy and Bhas-karan, 2017). Clearly, the aboveground portion of mangroves can directly dampen waves through their structural presence with sediment stabilization over soil (Gedan et al., 2011). Sediment carried by currents and waves provides important sediment material for mangrove tidal flat deposition (Long et al., 2022). The

Foundation item: The National Natural Science Key Foundation of China under contract No. 41930537; the Key Research Base of Humanities and Social Sciences in Guangxi Universities “Beibu Gulf Ocean Development Research Center” under contract No. 10BHZKY2110; the Key Research and Development Plan of Guangxi under contract No. Guike AB21076016; the Marine Science Program for Guangxi First-Class Discipline, Beibu Gulf University.

*Corresponding author, E-mail: zjdai@sklec.ecnu.edu.cn; mrhuanghu@126.com

attenuation difference is caused by the plant drag effect rather than bottom friction, and the wave damping rate is determined by the distance of the wave propagating along a mangrove band, which can allow much sediment to settle, thus promoting mangrove growth (Zhou et al., 2022). Moreover, some models have indicated that the biomechanical or hydrodynamic conditions of vegetation in mangroves can effectively dampen wave energy (Vo-Luong and Massel, 2008). Therefore, understanding mangrove biomorphodynamics is urgent for further ecosystem restoration and nature-based coastal protection. However, little information is known about the change in vegetation structures in mangroves, even though mangrove wetland dynamics have received exceptional attention worldwide.

The habitat environment is an important factor for the survival of mangrove ecosystems. Some studies have indicated that there are distinct characteristics in mangrove species composition, spatial structure, and distribution patterns of communities due to impacts from temperature, salt tolerance, and soil pH (Wang et al., 2021; Reyes, 2021; Qureshi et al., 2020). However, the ecological structure of mangrove forests is also determined by sediment grain size and heavy metal enrichment (Bhangle et al., 2021). Recent work has further shown, via remote images, that mangroves in Bangladesh have great ecological benefits to communities due to their structure (Hossain et al., 2021). Moreover, a recent study also revealed that plastic waste induced changes in the species composition and structure of mangrove forests in Jakarta (Rumondang et al., 2022). Surface elevation beneath mangroves can also be responsible for zonation of mangrove flora and fauna (Ma et al., 2020). Wang et al. (2019) found that there are close relations between mangrove community structure and the dynamics of sediment organic carbon. Moreover, most work has shown that morphological differences in vegetation patterns widely occur in various ecosystems, such as regular patch patterns (Klausmeier, 1999; Lejeune et al., 2002; Kéfi et al., 2010), banded patterns (Rietkerk et al., 2004), and complex maze or dot patterns (Eppinga et al., 2008; Casey et al., 2015; Getzin et al., 2016). Notably, the agglomerated structure of wetlands in coastal zones is a typical phenomenon, which can be employed as a strategy for wetland resilience to environmental stress (van de Koppel and Crain, 2006). Growth by agglomera-

tion in wetland plants can greatly weaken the hydrodynamics and promote the accumulation of sediments; this type of growth is also beneficial to plant colonization, as nutrients that accumulate in sediments further enhance plant survival (Temmerman et al., 2005; D'Alpaos, 2011; Belliard et al., 2016; FitzGerald and Hughes, 2019; Hu et al., 2021). However, little work has been done on the formation of mangrove community structure, especially on the horizontal structure characteristics of native mangrove species in the northern Beibu Gulf of China.

We know that plants block water flow and dissipate wave energy through morphological resistance and stem movement (Möller et al., 2014) to accelerate sediment deposition. Then, in the process of silting into the sea, the muddy sediment layer of the tidal flat gradually thickens (Yang et al., 2020), providing a new living space for mangroves.

Aegiceras corniculatum, a pioneer species of mangroves, is widely distributed along the northern Beibu Gulf of China (Long et al., 2022) and is mainly composed of a simple community with a single species or few species, such as *Kandelia candel*, *Sonneratia apetala* and *Acanthus ebracteatus* (Fig. 1). *Aegiceras corniculatum*, often used to restore mangrove wetlands in this region due to its aboriginal features and survival rate, presents different horizontal structures from seedlings to maturity. Therefore, the horizontal structure of *A. corniculatum* in the Nanliu Delta, the largest delta of the northern Beibu Gulf in China, was analyzed via ecological quadrats. The main aims of this study were to (1) examine the natural vegetation distribution of *A. corniculatum* from seedling to adult, (2) diagnose the change process of the horizontal structure in *A. corniculatum*, and (3) discern the main drivers affecting the horizontal structure of *A. corniculatum*.

2 Research area

The Nanliu Delta is the largest delta in the Beibu Gulf and covers an area of 550 km² with over 45% of mangrove forests along the northern Beibu Gulf; its estuary is divided into five branches in the Lianzhou Bay (Fig. 1). The tides in this area are irregular diurnal tides, with an average tidal range of approximately 2.5 m. Meanwhile, the dominant waves are northern and southwestern in the winter half-year and summer half-year, respectively. An average wave height of approximately 0.3 m is typ-

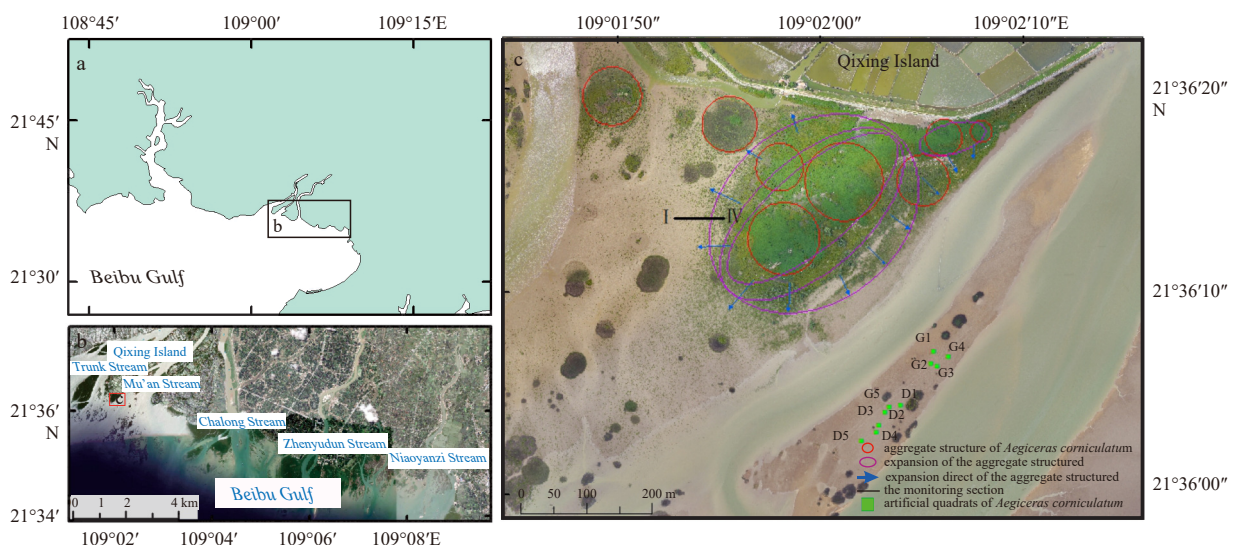


Fig. 1. The study area and the experimental design, location of the study area (a), Nanliu Delta (b), the experimental site of Nanliu Delta (c).

ical year-round (Long et al., 2022). *Aegiceras corniculatum*, with an area of 1 300 hm², is the main mangrove species distributed in the tidal flats of the five branches along the Nanliu Delta (Long et al., 2022) (Fig. 1).

The study area is located at the tail tidal flat of Qixing Island, which is between the Trunk Stream and the Mu'an Stream of the Nanliu River. Approximately 10 hm² of *A. corniculatum* is distributed over Qixing Island. There is approximately 10 hm² of bare beach in front of the mangrove forest, which is covered by sparse one- or two-year-old seedlings of *A. corniculatum*. Moreover, *Cyperus alaccensis* clusters are fragmentally scattered over the beach (Fig. 1).

3 Experimental design

Qixing Island is the largest fluvial island of the Nanliu Delta (Fig. 1b) and presents large-scale *A. corniculatum* from seedlings to adults over a seaward tidal flat. Here, three experiments were designed in the same wetland to analyze the formation of the agglomerated structure of *A. corniculatum* as follows.

3.1 Decomposition of UAV orthophoto and remote sensing image data

In July 2020, the tail tidal flat of Qixing Island was aerially photographed by a composite wing vertical take-off and landing drone equipped with a Sony 5100 camera. The flying height of the UAV was 250 m with a course overlap rate of 80%, a side overlap rate of 70%, and a ground resolution of 5 cm. Information about the distributed area, vegetation structure, and species of mangroves was interpreted by UAV images with validation of field observations (Fig. 1c). Furthermore, field investigations, unmanned aerial vehicles, and multiyear historical remote images (from the Google historical images of LocaSpace 4.0, with a resolution of 1.111 m) were combined to discern changes in mangrove ecological structures between 2000 and 2020. Moreover, a monitoring section was set with a field survey for investigating vegetation status (e.g., mangrove ages, configuration) to examine changes in horizontal structures on a spatial scale.

3.2 Analysis of grain size in sediments and nutrient elements

To explore the deposition effect of agglomerated structure (G) and discrete structure (D), the G and D quadrat comparative experiments were designed with 5 replicates, and the quadrats were distributed randomly on the bare beach in this study area to ensure the credibility of the experimental results. On October 5, 2020, G and D quadrats with areas of 5 m×5 m (Fig. 2) were designed on the bare intertidal zone of Qixing Island, separated

from the mangroves by a tidal creek (Fig. 1). The agglomerated forest structure comprised mangroves for which the distance between two adjacent plants was less than 1/10 of the height or canopy diameter of the seedlings; the discrete forest structure comprised mangroves for which this distance was greater than 1/10 of the height or canopy diameter of the seedlings. Then, 2-year-old seedlings of *A. corniculatum* with 40 were planted in these quadrats (Fig. 2).

Meanwhile, 500 g of surface sediment with a thickness of less than 1 cm was collected at five points evenly distributed on the diagonal of the quadrats on October 5, 2020 (Fig. 2). Subsequently, the corresponding surface sediment samples were collected again on January 8, 2022. Furthermore, 200 g sediment samples were used for particle size analysis using a Malvin 3000, and 300 g samples were used for laboratory analysis of nutrient elements, including total nitrogen (TN), total phosphorus (TP), and total potassium (TK), based on KJELTEC8400, UV 2600, and FP6410, respectively. Moreover, average values of grain size (D_{x50}), TN, TP, and TK in sediments at each point by five repetitions of each quadrat were used to represent the complete characteristics in deposition and nutrients of G and D.

3.3 Vegetation parameter collection of each quadrat

The height (H) and crown width (P) of each seedling in the quadrat were measured on October 5, 2020 and January 8, 2022, respectively. Meanwhile, the number of surviving plants was counted. The mangrove Preservation Rate (PR) is the number of surviving plants as a percentage of the number of originally planted plants (Nurcahaya Khairany et al., 2022), in which PR is defined as follows:

$$PR = N_s / N_o, \quad (1)$$

where N_s is the number of mangrove survivors for each repetition on January 8, 2022, and N_o is the original mangrove number of 40 on October 5, 2020.

Both the growth rate of height (GRH) and growth rate of crown width (GRCW) for *A. corniculatum* from October 5, 2020 to January 8, 2022 are defined, respectively, as:

$$GRH = H_i / H_o, \quad (2)$$

$$GRCW = P_i / P_o, \quad (3)$$

where H_i and H_o are the average heights of five repetitions in each quadrat on October 5, 2020 and January 8, 2022, respectively, and P_i and P_o are the average crown widths of five repetitions in each quadrat on October 5, 2020 and January 8, 2022, respectively.

4 Results

4.1 Changes in the horizontal structure of the *A. corniculatum* forest

There were a few small clusters of *A. corniculatum* in this study area in 2005 (Fig. 3a), where the largest cluster area was 1 276.30 m² and the smallest cluster area was 44.88 m². Meanwhile, there were some discrete seedlings of *A. corniculatum* randomly distributed over the tidal flat. We found that the original cluster area in 2005 peripherally expanded; by 2009, a number of small clusters combined with seedlings and grown saplings with

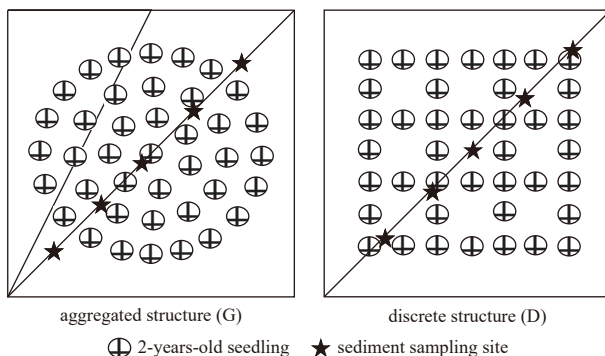


Fig. 2. Artificial quadrats with two different mangrove structures for the *Aegiceras corniculatum* population.

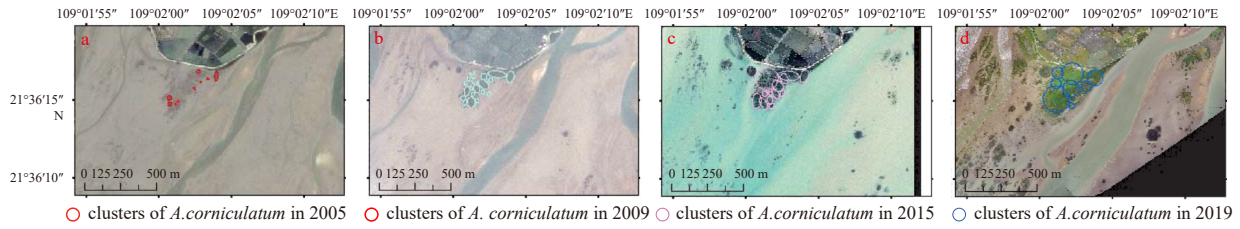


Fig. 3. Agglomeration formation process of *Aegiceras corniculatum*.

different sizes had grown by infilling sparse gaps among the previous clusters (Fig. 3b). Between 2009 and 2015, most grown clusters of *A. corniculatum* were further combined into several large agglomerations due to infilling from the expansion of grown seedlings, where new seedlings formed in the sparse gaps and sapling cluster structures again grew (Fig. 3c). Moreover, the orthographic image of the UAV in 2019 showed that the formed *A. corniculatum* clusters with mixtures of different ages in 2015 had been united into an adult ensemble with an oval configuration, which had a total area of 10.92 hm². In addition, there were a large number of *A. corniculatum* seedlings spread outside the forest edge of this oval ensemble cluster (Fig. 3d).

Furthermore, while an evolutionary pattern from a discrete to agglomerated structure of *A. corniculatum* by infillings can be found from 2005 to 2019 (Fig. 3), similarly dramatic variations in spatial scale also occurred in this study (Fig. 4). By analyzing four 5×5 m² quarters from sea to land along the set monitoring section, a field survey in October 2021 and auxiliary interpretation of UAV images in July 2020 (Figs 1 and 4a) found some discretely distributed *A. corniculatum* seedlings of approximately one or two years' age over seaward area I, which is far from the center of the large agglomerated clusters in area IV (Figs 4a, b-I). Area II consisted mainly of clusters of two-year-old seedlings with epis-

odically discrete distribution, which had been randomly infilled by one-year-old seedlings (Fig. 4b-II). However, there was a related sparse crown of *A. corniculatum*, which consisted mainly of saplings ranging from 3–5 years with mosaics of one or two seedlings (Fig. 4b-III). In addition, landward area IV had *A. corniculatum* over 5 years of age, which was almost fully occupied in most parts by related stable agglomerated clusters and dense forest forms (Fig. 4b-IV).

4.2 Vegetation growth in *A. corniculatum* quadrats

On October 5, 2020, 40 two-year seedlings of *A. corniculatum* were planted in quadrats G and D with 5 repetitions. On January 8, 2022, 38 seedlings in the G quadrats remained (Table 1), with a PR of 95.0% (Table 2), while 32 seedlings in the D quadrats remained (Table 1), with a PR of 80% (Table 2), indicating that the PR of the G quadrats was higher than that of the D quadrats.

Similarly, between October 2020 and January 2022, the average height of the G quadrats increased by 6.0 cm (Table 1), with a GRH of 17.86% (Table 2). The average crown width increased by 9.7 cm, with a GRCW increase of 55.11% (Table 2). However, after one year, the average height of seedlings in the D quadrats increased by 2.4 cm, with a GRH of 6.38% (Table 2). The average crown width increased by 15.5 cm, with a GRCW of 106.16% (Ta-

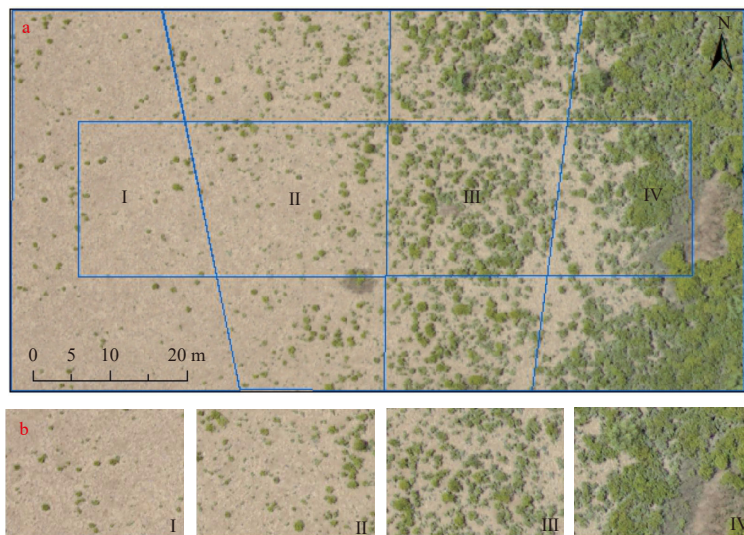


Fig. 4. Agglomerated structure development characteristics of *Aegiceras corniculatum*. a. Sections I–IV on the tidal flat of Qixing Island; b. agglomerated structure development process of *A. corniculatum*.

Table 1. Comparison of plant growth between the G and D quadrats

	G quadrats			D quadrats		
	Number of plants (N)	Average plant height (H)/cm	Average crown width (P)/cm	Number of plants (N)	Average plant height (H)/cm	Average crown width (P)/cm
2020-10-05	40	33.6	17.6	40	37.6	14.6
2022-01-08	38	39.6	27.3	32	40.0	30.1

Table 2. Comparison of GR and PR between the G and D quadrats

	G quadrats			D quadrats		
	Number of plants (N)	Average plant height (H)	Average crown width (P)	Number of plants (N)	Average plant height (H)	Average crown width (P)
GR/%		17.86	55.11		6.38	106.16
PR/%	95.0			80		

ble 1). Clearly, the height growth in seedlings of G quadrats was larger than that of D quadrats, while the crown width growth in seedlings of G quadrats was less than that of D quadrats.

Furthermore, on January 8, 2022, most seedlings in the D quadrats were entangled by *Enteromorpha prolifera*, while few seedlings in the G quadrats were surrounded by it (Figs 5a, b). The amount of *E. prolifera* in the G quadrats was smaller than that in the D quadrats (Fig. 5). This difference indicates that the seedlings grown in the G quadrats had stronger resistance to impacts from *E. prolifera* than those grown in the D quadrats, and seedling growth in the G quadrats was clearly better than that in the D quadrats. Moreover, in January 2022, *A. corniculatum* in the G quadrats again germinated new shoots, for which the growth length reached 5 cm (Fig. 5c), while the seedlings in the D quadrats showed almost no change in growth (Fig. 5d).

4.3 Grain size characteristics and nutrients in sediments beneath *A. corniculatum* quadrats

The mean grain sizes in the sediments of the G and D quadrats collected in October 2020 were 72.26 μm and 95.95 μm , respectively. The mean grain sizes in sediments collected in January 2022 from the G and D quadrats were 68.02 μm and 76.47 μm , respectively (Table 3). Clearly, the mean grain size in the sediments of these two quadrats after one year was much finer than that in the last year. Furthermore, the mean grain size in the sediment of the G quadrats was also finer than that of the D quadrats.

The *t* test shows that $P_{20}=0.002$, while $P_{21}=0.001$. Hence, there was a significant difference between the D_x (50) of sediment in the G and D quadrats in both 2020 and 2021. However, the standard error (δ) of the mean was 4.10 and 1.25 in the G and D quadrats in 2021, respectively, indicating that the sediment was more

homogeneous in 2021 in the G quadrats than in the D quadrats.

In comparison with those in the previous year, the TN and TP contents decreased clearly, while TK increased slightly in the sediment beneath *A. corniculatum* in the G and D quadrats (Table 4). In particular, TN decreased by approximately 0.015 g/kg in the G quadrat, while it decreased by 0.003 g/kg in only the D quadrat from 2020 to 2021. The TP content of the two quadrats decreased by approximately 0.01 g/kg (Table 4).

A *t* test showed that there was no significant difference between the TN, TP and TK contents in the G and D quadrats in both 2020 and 2021. However, the standard error (δ) of TN in 2020 was larger than that in 2021, while the standard error (δ) of TP and TK in 2020 was smaller than that in 2021.

5 Discussion

5.1 Impact of sedimentary dynamics

Some studies have indicated that mangroves can accelerate the deposition of suspended sediment in water bodies by slowing hydrodynamic forces and further promoting tidal flat silting (Shih and Cheng, 2022). Conversely, the promoted elevation of the tidal flat can benefit seedlings grown by increasing survival rates due to the actions of wave-tidal energy. In this study, the mean grain size in sediments beneath seedlings of *A. corniculatum* with D quadrats and G quadrats exhibited an increase in fine sediments from October 2020 to January 2022, indicating that seedlings subjected to the suspended sediment rapidly settled (Table 3). However, the mean grain size in sediments in quadrat D was much larger than that in quadrat G (Table 3), indicating that the ability of seedlings in quadrat G to promote elevation with fine suspended sediment deposition was much bet-



Fig. 5. Vegetation growth between agglomerated and discrete ecological quadrats, quadrat G in October 2020 (a), quadrat D in 2020 (b), quadrat G in January 2022 (c), quadrat D in January 2022 (d). Photos a and b taken on October 5, 2020, Photos c and d taken on January 8, 2022.

Table 3. Comparison of the mean grain size of the sediment between quadrats G and D

	G quadrats/ μm	D quadrats/ μm
2020-10-05	72.26 \pm 5.13	95.95 \pm 3.89
2022-01-08	68.02 \pm 1.56	76.47 \pm 2.04

ter than that in quadrat D.

In other words, an agglomerated structure for mangroves (e.g., G type) can effectively slow wave-current energy with rapid settling of suspended sediment, which can promote the elevation of tidal flats and benefit seedling survival. Meanwhile, the promoted tidal flat elevation can provide sufficient space for propagule implantation. The agglomerated structure can be further agglomerated with propagule growth, which will spread over the tidal flat in the future due to the intensive resilience of their structures against wave-current actions.

5.2 Changes in nutrient contents in sediments

Compared with 2020, in 2021, the TK contents in sediments of both D quadrats and G quadrats increased noticeably (Table 4), demonstrating that the *A. corniculatum* forest can promote the enrichment of TK via absorption of fine particulate matter. Meanwhile, the sediments are finer and the TK contents are higher in the G quadrats than in the D quadrats. This difference could be attributed to the fact that relatively fine sediment can absorb much more TK, and the agglomerated clusters can deposit much finer sediment than the discrete structure. Thereafter, higher contents of TK in sediments of G quadrats are more beneficial to seedling growth than those of D quadrats. Our results, which showed that the mangrove preservation rate in agglomerated quadrats is much higher than that in discrete quadrats, also further demonstrate the significance of agglomeration for mangrove survival.

In contrast, the TN and TP contents of the sediment in these two quadrats in 2021 were lower than those in the previous year (Table 4). At the same time, the TN and TP contents of the sediment in the G quadrats decreased more than those in the D quadrats. N mostly exists in water in the form of NH_4^+ and NO_3^- and adheres to microparticles (Chiban et al., 2016), while P is

formed by soluble phosphorus (DP), iron-bound phosphorus (Fe-P), aluminum-bound phosphorus (Al-P), calcium-bound phosphorus (Ca-P) and organic phosphorus (OP) (Ma et al., 2022).

Furthermore, while NH_4^+ in surface sediments is volatilized, NO_3^- can infiltrate into the soil with water after the ebb tide period. This means that N does not easily accumulate within surface sediments. Moreover, the *A. corniculatum* seedlings vigorously grew in summer and autumn, consuming a large amount of N. The more vigorously the seedlings grew, the more N element they consumed. In brief, the *A. corniculatum* seedlings that grew together within G quadrats were better than those within D quadrats, and they consumed more N than those within D quadrats. Therefore, the TN content decreased in the G quadrats more than in the D quadrats. Additionally, P infiltrates the water during ebb tide, and P is absorbed by seedlings during the growing season, which might be the primary cause of the decrease in TP from 2020 to 2021.

Overall, the *A. corniculatum* forest can accelerate the process of microparticle deposition by slowing hydrodynamic forces, promoting the enrichment of nutrient elements in sediments for plant growth. Moreover, the ecological function of the agglomerated structure was stronger than that of the discrete structure, which further promoted the development of forest structure.

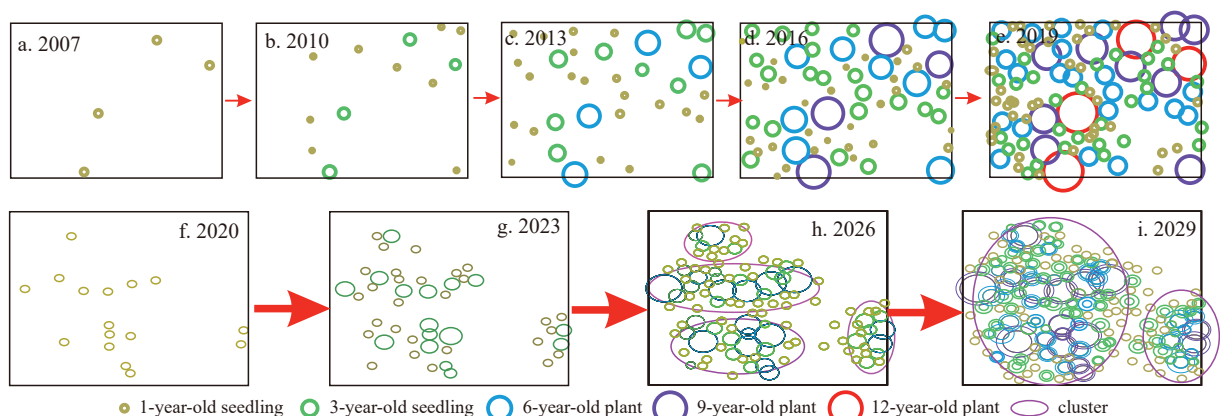
5.3 Evolution patterns of horizontal structure for the *A. corniculatum* population

The horizontal structure of mangroves is affected by multiple factors (FitzGerald and Hughes, 2019), which could be mainly determined by the growth rate of mangrove seedlings (Kusmana and Azizah, 2022). Here, based on an image interpreted by UAV (Fig. 4b-IV) in combination with a field survey, the basic evolution patterns of the horizontal structure for the *A. corniculatum* population in the Nanliu River estuary can be summarized as follows (Fig. 6).

According to the age of each plant in quadrat IV (Fig. 4b-IV), the distribution status of *A. corniculatum* in each year can be inverted. There were only 4 current-year viviparous seedlings distributed discretely in quadrat IV in 2007 (Fig. 6a). By 2010, we

Table 4. Comparison of the nutritive element contents of the sediment between the G and D quadrats

	G quadrats			D quadrats		
	TN content/(g·kg ⁻¹)	TP content/(g·kg ⁻¹)	TK content/(g·kg ⁻¹)	TN content/(g·kg ⁻¹)	TP content/(g·kg ⁻¹)	TK content/(g·kg ⁻¹)
2020-10-08	0.081 \pm 0.051	0.046 \pm 0.001	0.908 \pm 0.039	0.065 \pm 0.005	0.045 \pm 0.002	0.856 \pm 0.055
2021-10-11	0.066 \pm 0.008	0.034 \pm 0.07	1.049 \pm 0.030	0.062 \pm 0.007	0.035 \pm 0.004	0.998 \pm 0.074

**Fig. 6.** Evolution patterns for the aggregated structure of *Aegiceras corniculatum*.

found that the original 4 seedlings gradually grew after 3 years of growth and development, and new current-year seedlings filled. The number of plants in quadrat IV increased, but the distribution was still discrete (Fig. 6b). By 2013, the previous 2007 seedlings had grown to 6 years old, and the previous 2010 seedlings had grown to 3 years old. Subsequently, the new seedlings were filled in 2013, while the previous seedlings in 2007 and 2010 had grown. The number of plants in quadrat IV increased, but the distribution of *A. corniculatum* was still discrete (Fig. 6c). Similarly, from 2013 to 2016, the plants were persistently grown, new plants were sustainably filled, and small agglomerations were formed (Fig. 6d). Meanwhile, it occurred again in 2019, and the agglomerated structure was built in quadrat IV (Fig. 6e).

Taken together, the developing law of *A. corniculatum* forest in quadrat IV showed that with increasing age, the plants grew and new seedlings filled continuously, and the discrete structure of *A. corniculatum* in the early stage gradually developed into an agglomerated structure (Figs 6a–e).

Furthermore, based on the abovementioned developmental law of mangroves from a discrete structure to an agglomerated structure between 2007 and 2019, we can infer the possible status of seedlings in quadrat I in the future (Fig. 4b–I). The discrete seedlings in 2020 will grow and develop (Fig. 6f), and new seedlings will fill in continuously between plants in 2023 (Fig. 6g), so the seedlings will aggregate gradually into small clusters in 2026 (Fig. 6h). With further growth and filling, the small clusters aggregate into large clusters in 2029 (Fig. 6i).

5.4 Prospective

Aegiceras corniculatum grows at the front of the tidal flat, which can be washed by frequent tides or episodic storm surges. The scattered plants were gradually eliminated due to long-term impacts from harsh environments (Ghazian et al., 2021). However, the ecological quadrat monitoring of the two structures revealed that the agglomerated structure was more conducive to plant growth and community development. The preservation rate and growth potential of plants in the agglomerated structure were much higher than those in the discrete structure (Fig. 5). In this experiment, the increment of crown width of the discrete structure was larger than that of the agglomerated structure (Fig. 5). The greater distance between discrete structure plants gives the plants more room to develop and benefits branch relaxation (Ghazian et al., 2021). This growth also shows that the discrete structure was developing toward the agglomerated structure for *A. corniculatum*. Clearly, agglomerated structures should be preferentially selected for mangrove restoration, as they can enhance the resistance of mangroves to external stress and greatly improve their survival rate.

6 Conclusions

A reasonable horizontal structure plays an important role in mangrove conservation and ecological restoration. In this study, the horizontal structure of the *A. corniculatum* population was investigated based on the natural mangrove population in the tidal flat of the Nanliu Delta, and artificially agglomerated and discrete ecological quadrats were set up to interpret the driving mechanism of agglomerated structure formation. The main conclusions are as follows:

(1) Agglomerated and discrete structures occurred in the *A. corniculatum* forest. These two structures can be found in seedlings and saplings of *A. corniculatum*, while agglomerated structures are mainly found in adult *A. corniculatum*. The discrete structure of *A. corniculatum* will evolve into an agglomerated

structure due to the impacts of complicated natural forcing.

(2) Agglomerated structures can weaken the hydrodynamic force, attenuate the grain size of sediments and accelerate deposition, which is beneficial for promoting the elevation of tidal flats by providing favorable conditions for the landing of *A. corniculatum* embryos.

(3) Compared with the discrete structure, the agglomerated structure is conducive to the accumulation of nutrients such as TN, TP and TK, which provide nutritional guarantees for plant growth and population development. It can be expected that agglomerated structures designed for seedling planting will greatly benefit mangrove restoration.

References

- Belliard J P, Di Marco N, Carniello L, et al. 2016. Sediment and vegetation spatial dynamics facing sea-level rise in microtidal salt marshes: Insights from an ecogeomorphic model. *Advances in Water Resources*, 93: 249–264, doi: [10.1016/j.advwatres.2015.11.020](https://doi.org/10.1016/j.advwatres.2015.11.020)
- Bhangle P P, Nayak G N, Choudhary S. 2021. Processes and metal enrichment of adjacent mudflat and mangrove environments in the middle estuarine regions of tropical Mandovi Estuary, Goa, west coast of India. *Environmental Earth Sciences*, 80(16): 530, doi: [10.1007/S12665-021-09853-7](https://doi.org/10.1007/S12665-021-09853-7)
- Casey S T, Cohen M J, Acharya S, et al. 2015. On the spatial organization of the ridge slough patterned landscape. *Hydrology and Earth System Sciences Discussions*, 12(3): 2975–3010
- Chiban M, Carja G, Lehtu G, et al. 2016. Equilibrium and thermodynamic studies for the removal of As(V) ions from aqueous solution using dried plants as adsorbents. *Arabian Journal of Chemistry*, 9(S2): S988–S999, doi: [10.1016/j.arabjc.2011.10.002](https://doi.org/10.1016/j.arabjc.2011.10.002)
- D'Alpaos, 2011. The mutual influence of biotic and abiotic components on the long-term ecomorphodynamic evolution of salt-marsh ecosystems. *Geomorphology*, 126(3–4): 269–278
- Danielsen F, Sørensen M K, Olwig M F, et al. 2005. The Asian Tsunami: A protective role for coastal vegetation. *Science*, 310(5748): 643, doi: [10.1126/science.1118387](https://doi.org/10.1126/science.1118387)
- Eppinga M B, Rietkerk M, Borren W, et al. 2008. Regular surface patterning of peatlands: Confronting theory with field data. *Ecosystems*, 11(4): 520–536, doi: [10.1007/s10021-008-9138-z](https://doi.org/10.1007/s10021-008-9138-z)
- FAO. 2020. Global Forest Resources Assessment 2020: Main report. Rome: FAO
- FitzGerald D M, Hughes Z. 2019. Marsh processes and their response to climate change and sea-level rise. *Annual Review of Earth and Planetary Sciences*, 47: 481–517, doi: [10.1146/annurev-earth-082517-010255](https://doi.org/10.1146/annurev-earth-082517-010255)
- Friess D A, Rogers K, Lovelock C E, et al. 2019. The State of the world's mangrove forests: Past, present, and future. *Annual Review of Environment and Resources*, 44: 89–115, doi: [10.1146/annurev-environ-101718-033302](https://doi.org/10.1146/annurev-environ-101718-033302)
- Gedan K B, Kirwan M L, Wolanski E, et al. 2011. The present and future role of coastal wetland vegetation in protecting shorelines: answering recent challenges to the paradigm. *Climatic Change*, 106(1): 7–29, doi: [10.1007/s10584-010-0003-7](https://doi.org/10.1007/s10584-010-0003-7)
- Getzin S, Yizhaq H, Bell B, et al. 2016. Discovery of fairy circles in Australia supports self-organization theory. *Proceedings of the National Academy of Sciences of the United States of America*, 113(13): 3551–3556, doi: [10.1073/pnas.1522130113](https://doi.org/10.1073/pnas.1522130113)
- Ghazian N, Braun J, Owen M, et al. 2021. Seed aggregation tips the scale in plant competition. *Community Ecology*, 22(3): 403–412, doi: [10.1007/S42974-021-00064-5](https://doi.org/10.1007/S42974-021-00064-5)
- Hossain M S, Hossain M B, Rakib M R J, et al. 2021. Ecological and human health risk evaluation using pollution indices: A case study of the largest mangrove ecosystem of Bangladesh. *Regional Studies in Marine Science*, 47: 101913, doi: [10.1016/J.RSMA.2021.101913](https://doi.org/10.1016/J.RSMA.2021.101913)
- Hu Zhan, Borsje B W, van Belzen J, et al. 2021. Mechanistic modeling of marsh seedling establishment provides a positive outlook for coastal wetland restoration under global climate change. *Geo-*

- physical Research Letters, 48(22): e2021GL095596
- Kéfi S, Eppinga M B, de Ruiter P C, et al. 2010. Bistability and regular spatial patterns in arid ecosystems. *Theoretical Ecology*, 3(4): 257–269, doi: [10.1007/s12080-009-0067-z](https://doi.org/10.1007/s12080-009-0067-z)
- Klausmeier C A. 1999. Regular and irregular patterns in semiarid vegetation. *Science*, 284(5421): 1826–1828, doi: [10.1126/science.284.5421.1826](https://doi.org/10.1126/science.284.5421.1826)
- Kusmana C, Azizah N A. 2022. Species composition and Vegetation Structure of Mangrove Forest in Pulau Rambut Wildlife Reserve, Kepulauan Seribu, DKI Jakarta. *IOP Conference Series: Earth and Environmental Science*, 950(1): 012020, doi: [10.1088/1755-1315/950/1/012020](https://doi.org/10.1088/1755-1315/950/1/012020)
- Lejeune O, Thidi M, Couteron P. 2002. Localized vegetation patches: A self-organized response to resource scarcity. *Physical Review E*, 66(1): 010901, doi: [10.1103/PhysRevE.66.010901](https://doi.org/10.1103/PhysRevE.66.010901)
- Long Chuqi, Dai Zhijun, Wang Riming, et al. 2022. Dynamic changes in mangroves of the largest delta in northern Beibu Gulf, China: Reasons and causes. *Forest Ecology and Management*, 504: 119855, doi: [10.1016/j.foreco.2021.119855](https://doi.org/10.1016/j.foreco.2021.119855)
- Long Chuqi, Dai Zhijun, Zhou Xiaoyan, et al. 2021. Mapping mangrove forests in the Red River Delta, Vietnam. *Forest Ecology and Management*, 483: 118910, doi: [10.1016/j.foreco.2020.118910](https://doi.org/10.1016/j.foreco.2020.118910)
- Lovelock C E, Cahoon D R, Friess D A, et al. 2015. The vulnerability of Indo-Pacific mangrove forests to sea-level rise. *Nature*, 526(7574): 559–563, doi: [10.1038/nature15538](https://doi.org/10.1038/nature15538)
- Lovelock C E, Feller I C, Reef R, et al. 2017. Mangrove dieback during fluctuating sea levels. *Scientific Reports*, 7(1): 1680, doi: [10.1038/s41598-017-01927-6](https://doi.org/10.1038/s41598-017-01927-6)
- Ma Wei, Wang Wenqing, Tang Chaoyi, et al. 2020. Zonation of mangrove flora and fauna in a subtropical estuarine wetland based on surface elevation. *Ecology and Evolution*, 10(14): 7404–7418, doi: [10.1002/ece3.6467](https://doi.org/10.1002/ece3.6467)
- Ma Huihui, Zhu Yuanrong, Jiang Juan, et al. 2022. Characteristics of inorganic and organic phosphorus in Lake Sha sediments from a semiarid region, Northwest China: Sources and bioavailability. *Applied Geochemistry*, 137: 105209, doi: [10.1016/j.apgeochem.2022.105209](https://doi.org/10.1016/j.apgeochem.2022.105209)
- Mishra M, Acharyya T, Santos C A G, et al. 2021. Geo-ecological impact assessment of severe cyclonic storm Amphan on Sundarban mangrove forest using geospatial technology. *Estuarine, Coastal and Shelf Science*, 260: 107486, doi: [10.1016/j.ecss.2021.107486](https://doi.org/10.1016/j.ecss.2021.107486)
- Möller I, Kudella M, Rupprecht F, et al. 2014. Wave attenuation over coastal salt marshes under storm surge conditions. *Nature Geoscience*, 7(10): 727–731, doi: [10.1038/ngeo2251](https://doi.org/10.1038/ngeo2251)
- Nurchahaya Khairany M A, Farah Shahanim M M, Zahirah M T. 2022. In situ conservation of mangroves species in Bagan Datuk, Perak. *IOP Conference Series: Earth and Environmental Science*, 1053(1): 012009, doi: [10.1088/1755-1315/1053/1/012009](https://doi.org/10.1088/1755-1315/1053/1/012009)
- Parvathy K G, Bhaskaran P K. 2017. Wave attenuation in presence of mangroves: A sensitivity study for varying bottom slopes. *International Journal of Ocean and Climate Systems*, 8(3): 126–134, doi: [10.1177/1759313117702919](https://doi.org/10.1177/1759313117702919)
- Qureshi K A, Seroor M, Al-Masabi A, et al. 2020. Bio-characterizations of some marine bacterial strains isolated from mangrove sediment samples of four major cities of Saudi Arabia. *The Journal of Environmental Biology*, 41(5): 1003–1012, doi: [10.22438/JEB/41/5/MRN-1317](https://doi.org/10.22438/JEB/41/5/MRN-1317)
- Reyes P A M D. 2021. Species distribution and abundance of mangrove species in different Zonation of Bayabas, Surigao del Sur, Philippines. *Journal of Biodiversity & Endangered Species*, 9(7): 1–3
- Rietkerk M, Dekker S C, de Ruiter P C, et al. 2004. Self-organized patchiness and catastrophic shifts in ecosystems. *Science*, 305(5692): 1926–1929, doi: [10.1126/science.1101867](https://doi.org/10.1126/science.1101867)
- Rumondang A L, Kusmana C, Budi S W. 2022. Species composition and structure of mangrove forest exposed to plastic waste in Angke Kapuk mangrove protected forest, Jakarta. *IOP Conference Series: Earth and Environmental Science*, 950(1): 012016, doi: [10.1088/1755-1315/950/1/012016](https://doi.org/10.1088/1755-1315/950/1/012016)
- Shih Shang-Shu, Cheng Ting-Yu. 2022. Geomorphological dynamics of tidal channels and flats in mangrove swamps. *Estuarine, Coastal and Shelf Science*, 265: 107704, doi: [10.1016/j.ecss.2021.107704](https://doi.org/10.1016/j.ecss.2021.107704)
- Temmerman S, Bouma T J, Govers G, et al. 2005. Impact of vegetation on flow routing and sedimentation patterns: Three-dimensional modeling for a tidal marsh. *Journal of Geophysical Research: Earth Surface*, 110(F4): F04019
- van de Koppel J, Crain C M. 2006. Scale-dependent inhibition drives regular tussock spacing in a freshwater marsh. *The American Naturalist*, 168(5): E136–E147, doi: [10.1086/508671](https://doi.org/10.1086/508671)
- Vo-Luong P, Massel S. 2008. Energy dissipation in non-uniform mangrove forests of arbitrary depth. *Journal of Marine Systems*, 74(1–2): 603–622
- Wang Gang, Guan Dongsheng, Xiao Ling, et al. 2019. Changes in mangrove community structures affecting sediment carbon content in Yingluo Bay of South China. *Marine Pollution Bulletin*, 149: 110581, doi: [10.1016/j.marpolbul.2019.110581](https://doi.org/10.1016/j.marpolbul.2019.110581)
- Wang Gang, Yu Chenxi, Singh M, et al. 2021. Community structure and ecosystem carbon stock dynamics along a chronosequence of mangrove plantations in China. *Plant and Soil*, 464(1–2): 605–620, doi: [10.1007/S11104-021-04973-2](https://doi.org/10.1007/S11104-021-04973-2)
- Woodroffe C D, Rogers K, McKee K L, et al. 2016. Mangrove sedimentation and response to relative sea-level rise. *Annual Review of Marine Science*, 8(1): 243–266, doi: [10.1146/annurev-marine-122414-034025](https://doi.org/10.1146/annurev-marine-122414-034025)
- Yang Shilun, Luo Xiangxin, Temmermans S, et al. 2020. Role of delta-front erosion in sustaining salt marshes under sea-level rise and fluvial sediment decline. *Limnology and Oceanography*, 65(9): 1990–2009, doi: [10.1002/lno.11432](https://doi.org/10.1002/lno.11432)
- Zhou Xiaoyan, Dai Zhijun, Pang Wenhong, et al. 2022. Wave attenuation over mangroves in the Nanliu Delta, China. *Frontiers in Marine Science*, 9: 874818, doi: [10.3389/fmars.2022.874818](https://doi.org/10.3389/fmars.2022.874818)